

Proteomics analysis of date palm leaves affected at three characteristic stages of brittle leaf disease

Besma Sghaier-Hammami · Mohammed Najib Saidi ·
M^a Ángeles Castillejo · Jesús V. Jorrín-Novo · Ahmed Namsi ·
Noureddine Drira · Radhia Gargouri-Bouزيد

Received: 19 April 2012 / Accepted: 10 July 2012 / Published online: 29 July 2012
© Springer-Verlag 2012

Abstract Proteomics analysis has been performed in leaf tissue from field date palm trees showing the brittle leaf disease (BLD) or *maladie des feuilles cassantes*, the main causal agent of the date palm decline in south Tunisia. To study the evolution of the disease, proteins from healthy and affected leaves taken at three disease stages (S1, S2 and S3) were trichloroacetic acid acetone extracted and subjected to two-dimensional gel electrophoresis (5–8 pH range). Statistical analysis showed that the protein abundance profile is different enough to differentiate the affected leaves from the

healthy ones. Fifty-eight variable spots were successfully identified by matrix-assisted laser desorption ionization time of flight, 60 % of which corresponded to chloroplastic ones being involved in the photosynthesis electronic chain and ATP synthesis, metabolic pathways implicated in the balance of the energy, and proteases. Changes in the proteome start at early disease stage (S1), and are greatest at S2. In addition to the degradation of the ribulose-1.5-bisphosphate carboxylase oxygenase in affected leaflets, proteins belonging to the photosynthesis electronic chain and ATP synthesis decreased following the disease, reinforcing the relationship between BLD and manganese deficiency. The manganese-stabilizing proteins 33 kDa, identified in the present work, can be considered as protein biomarkers of the disease, especially at early disease step.

B. Sghaier-Hammami and M. N. Saidi contributed equally to this work.

Electronic supplementary material The online version of this article (doi:10.1007/s00425-012-1713-z) contains supplementary material, which is available to authorized users.

B. Sghaier-Hammami (✉) · N. Drira
Laboratoire des Biotechnologies Végétales Appliquées à
l'Amélioration des Cultures, Faculté des Sciences de Sfax,
Route de Soukra km 4, B.P. 1171, 3018 Sfax, Tunisia
e-mail: sghaierbesma@yahoo.fr; rb2sosoh@uco.es

B. Sghaier-Hammami · J. V. Jorrín-Novo
Agricultural and Plant Biochemistry and Proteomics Research
Group, Department of Biochemistry and Molecular Biology,
University of Córdoba, ceiA3, 14071 Córdoba, Spain

M. N. Saidi · R. Gargouri-Bouزيد
Laboratoire des Biotechnologies Végétales Appliquées à
l'Amélioration des Cultures, Ecole Nationale d'Ingénieurs
de Sfax, Route Soukra km 4, B.P. 1173, 3038 Sfax, Tunisia

M. Á. Castillejo
Department of Molecular Systems Biology,
University of Vienna, 1090 Vienna, Austria

A. Namsi
Centre de Recherches Phoenicoles, 2260 Degache, Tunisia

Keywords Brittle leaf disease · Date palm proteomics ·
Manganese-stabilizing proteins · Proteases · RubisCO

Abbreviations

HC	Healthy control
IEF	Isoelectric focusing
MALDI	Matrix-assisted laser desorption ionization
MFC	Maladie des feuilles cassantes (brittle leaf disease)
MSP	Manganese-stabilizing proteins
TOF	Time of flight
RubisCO	Ribulose-1.5-bisphosphate carboxylase/oxygenase large subunit

Introduction

Date palm (*Phoenix dactylifera* L.) cultures in Tunisian oases suffer from a disease called brittle leaf disease

(BLD), known in French as *maladie des feuilles cassantes* (MFC), which became epidemic ever since 1980 (Triki et al. 2003) and has been reported in eastern Algeria (Saadi et al. 2006). The most characteristic symptom of the disease concerns the plant leaves that become brittle and break easily when flexed and squeezed. The disease evolution has been divided into three stages (1) the first one (S1) is characterized by chlorosis of a few fronds, (2) in the second stage (S2), leaflets become brittle, twisted and frizzled and (3) the symptoms extend in stage 3 (S3) to the entire plant that finally dies (Triki et al. 2003). Symptoms extend to the upper fronds until the whole plant becomes affected and stunted, stops growing, and finally dies (Triki et al. 2003). Although, the MFC epidemiology suggested a biotic etiology, so far no pathogen associated with the disease could be found (Triki et al. 2003). There are two main features of this disease: a manganese (Mn) deficiency in the leaflets of affected palms (Namsi et al. 2007) and the abnormal accumulation of a set of novel RNAs transcribed from the date palm chloroplast genome (Marqués et al. 2008).

Leaflets of affected palms have been shown to contain significantly lower Mn concentrations than those of healthy controls (Namsi et al. 2007). Soils in which MFC develops are Mn deficient and contain about half the manganese content compared to healthy soils (Namsi et al. 2007). Moreover, Mn is the only element for which significant differences are seen in adult leaflets between healthy trees and MFC-affected trees (Namsi et al. 2007). Transcriptomic analysis of MFC-affected leaves showed that a repression of manganese-related genes, photosynthesis, ion transport and protein synthesis occurred in affected leaves, while stress response, metabolism associated, protein synthesis and signal transduction genes were up-regulated by the disease (Saidi et al. 2010).

Manganese deficiency in green plants is known to affect preferentially the activity of the oxygen-evolving system in

the photosynthetic apparatus. Higher plants responded to manganese deficiency either by adjusting the number of chloroplasts per cell to the limited Mn supply, or by forming disorganized chloroplasts with low chlorophyll content (Homann 1967). Recently, at the proteomics level, Marqués et al. (2011) reported that Mn-binding PSBO and PSBP proteins, components of the oxygen-evolving complex of photosystem II, were decreased in affected date palm leaves not yet entering into final decline (leaves from stage S2).

The objective of this work is the characterization of the proteome changes that occur in date palm leaves affected by MFC disease from the beginning of the disease (stage S1) to the death of the palm trees (stage S3). In addition, we are interested in finding protein biomarkers of MFC disease that reinforce its relationship to Mn deficiency by studying the function of some identified proteins which may be a key in this disease.

Materials and methods

Plant material

Leaf tissues from field date palm (*Phoenix dactylifera* L. cv. Deglet Nour) trees (resulting from offshoot propagation) are used in the present work. The healthy and affected palm trees belong to the same cultivar. In the MFC-affected oasis (southern Tunisia; Degache), the following trees were selected: healthy control (HC), trees with mild (S1), moderate (S2), and severe (S3) symptoms. The three stages of MFC symptoms (S1, S2 and S3; Fig. 1) were identified and selected based on the symptoms as described by Triki et al. (2003). Four to six years may elapse between the appearance of the first symptoms (stage S1) and death of the tree (stage S3). HC leaflets were collected from the same oasis as that of the affected palm trees, but at

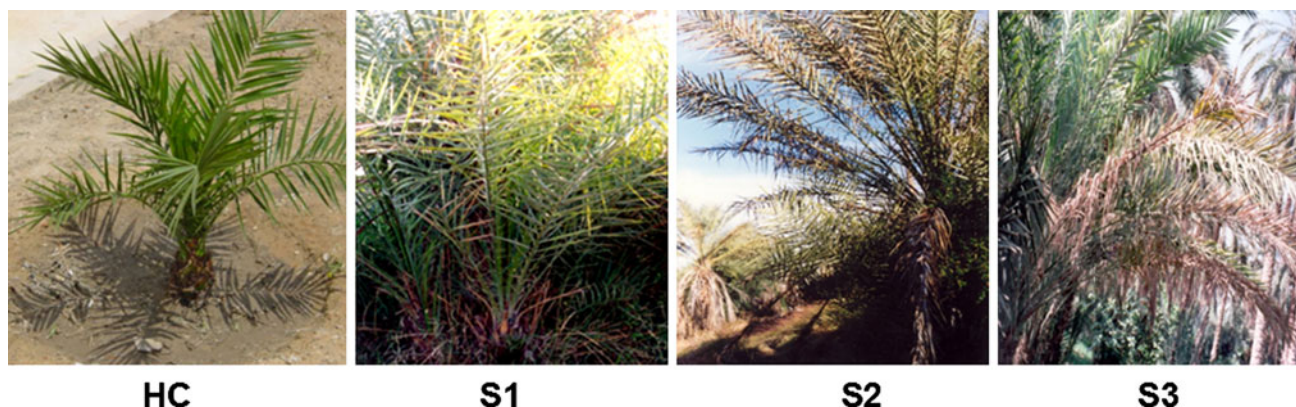


Fig. 1 A symptom of brittle leaf disease (*maladie des feuilles cassantes*) in date palm tree taken from different disease stages (S1, S2 and S3). HC, healthy control

different locations, where MFC symptoms have never been observed.

Protein extraction and 2-DE electrophoresis

Leaves (10 leaves per plant/one plant per replicate/three replicates) from healthy and affected trees were collected, thoroughly washed with water, dried with filter paper, frozen in liquid nitrogen, and stored at -80°C until protein extraction. Leaves were ground to a fine powder in liquid nitrogen using a mortar and pestle and the powder (0.5 g) was subjected to a TCA–acetone–phenol protein extraction procedure (Wang et al. 2006; Maldonado et al. 2008). The final pellet was dissolved in 40–200 μl of 7 M urea, 2 M thiourea, 4 % CHAPS and 100 mM DTT (Bio-Lyte 3/10, Bio-Rad). Once the pellet was solubilized and the insoluble material eliminated by centrifugation, the protein content was quantified by the method of Bradford (1976), using bovine serum albumin as standard.

For 2-DE, IPG strips (17 cm, 5–8 pH linear gradient; Bio-Rad) were passively rehydrated for 16 h with 400 μg protein in 300 μl of IEF solubilisation buffer [7 M urea; 2 M thiourea; 4 % (w/v) CHAPS; 0.2 % (v/v) IPG buffer 5–8, 100 mM DTT; and 0.01 % (w/v) bromophenol blue]. The strips were loaded onto a Bio-Rad Protean IEF cell system and proteins were electrofocused (Maldonado et al. 2008). Strips were equilibrated and subjected to second-dimension SDS-PAGE, then stained with Colloidal Coomassie Blue G-250 (Maldonado et al. 2008).

Images were digitized with a GS-800 calibrated densitometer (Bio-Rad) and analyzed with the PDQuestTM software (Bio-Rad), using a guided protein spot detection method (Chich et al. 2007). Normalized spot volumes based on total quantity in valid spots were calculated for each 2-DE gel and used for statistical evaluation of differential protein abundance. Experimental M_r values were calculated by mobility comparisons with molecular weight standards of low range (Bio-Rad) run in a separate marker lane on the SDS-gel, while pI was determined using a 5–8 linear scale over the total dimension of the IPG strips.

MS analysis and protein identification

Spots were automatically excised (Investigator ProPic, Genomic Solutions), transferred to Multiwell 96 plates and digested with modified porcine trypsin (sequencing grade; Promega) using a ProGest (Genomics Solution) digestion station. The digestion protocol used was that of Schevchenko et al. (1996), with minor variations. Gel plugs were destained by incubation (twice for 30 min) with 200 mM ammonium bicarbonate in 40 % acetonitrile (ACN) at 37°C , then subjected to three consecutive dehydration/rehydration cycles with pure ACN and 25 mM

ammonium bicarbonate in 40 % ACN, respectively, and finally dried at room temperature for 10 min. Trypsin (20 μl) at a final concentration of 12.5 ng/ μl in 25 mM ammonium bicarbonate was added to the dry gel pieces and the digestion proceeded at 37°C overnight.

Peptides were extracted from gel plugs by adding 10 μl of 1 % TFA (15 min incubation), and were then purified by ZipTip $\mu\text{-C}_{18}$ (Millipore). Peptides were deposited onto matrix-assisted laser desorption ionization (MALDI) plate using the dry droplet method (ProMS, Genomic Solutions) and the α -cyano hydroxycinnamic acid as a matrix at 5 $\mu\text{g}/\mu\text{l}$ concentration in 70 % ACN, 0.1 % TFA. Samples were analyzed in a 4700 Proteomics Analyzer MALDI-(TOF/TOF) Mass Spectrometer (Applied Biosystems), in the m/z range 800–4,000, with an accelerating voltage of 20 kV, in reflectron mode and with a delayed extraction set to 120 ns. Spectra were calibrated using the trypsin autolysis peaks at $m/z = 842.509$ and $m/z = 2211.104$ as internal standards. The three most abundant ions were then subjected to MS/MS analysis, providing information that could be used to determine the peptide sequence.

A combined search (MS plus MS/MS) was performed using GPS ExplorerTM software v 3.5 (Applied Biosystems) over NCBI Inr database using the MASCOT v 1.9 search engine (Matrix Science Ltd., London; <http://www.matrixscience.com>). The following parameters were allowed: taxonomy restrictions to Viridiplantae, one missed cleavage, 10 ppm mass tolerance in MS and 0.5 Da for MS/MS data, cysteine carbamidomethylation as a fixed modification and methionine oxidation as a variable modification. The confidence in the peptide mass fingerprinting matches ($P \leq 0.05$) was based on the MOWSE score and confirmed by the accurate overlapping of the matched peptides with the major peaks of the mass spectrum.

Statistical analysis

For statistical analysis, treatment and cluster analysis of protein abundance values, the web-based software NIA array analysis tool was utilized (Sharov et al. 2005) available at <http://lgsun.grc.nia.nih.gov/anova/index.html>. This software tool selects statistically valid protein spots based on analysis of variance (ANOVA). After uploading the data table (Supplementary Table 1) and indication of biological replications, the data were statistically analyzed using the following settings: error model max (average, actual), 0.01 proportions of highest variance values to be removed before variance averaging, 10 degrees of freedom for the Bayesian error model, 0.05 FDR threshold, and zero permutations.

The entire data set was analyzed by principal component analysis (PCA) using the following settings: covariance matrix type, four principal components, twofold change threshold for clusters, and 0.5 correlation threshold for

clusters. PCA results were represented as a biplot, with consistent proteins in those experimental situations located in the same area of the graph. To perform this statistical cluster analysis, a software tool designed for the analysis of biological gene chip data was used (Sharov et al. 2005), which has also been successfully employed in the analysis of protein abundance data (Brumbarova et al. 2008; Castillejo et al. 2010a, b; Sghaier-Hammami et al. 2012).

The identified proteins were subjected to heat mapping using Euclidean distance (Eisen et al. 1998), with average linkage algorithm of the Genesis software package allowing a definition of some expression groups, the presence or absence of some of them being a characteristic of a particular group (Sturn et al. 2002).

Results

Leaves collected from MFC-affected trees were verified as having symptoms, and the three stages of MFC symptoms (S1, S2 and S3) were selected as described by Triki et al.

(2003). Total proteins were extracted from HC and affected leaflets from the first symptoms of the disease (stage S1) to the death of the tree (stage S3, Fig. 1).

Protein extraction and 2-DE analysis

Proteins from HC and affected leaves at each disease stage (three biological replicates) were extracted based on TCA–acetone–phenol methods. The different protein samples (400 µg) were separated by 2-DE (Fig. 2) with IEF carried out in the 5–8 pH range. In all, 364 spots could be resolved in the master gel with most of them (297 spots) being variable between samples (affected leaves and HC). The total number of resolved spots increased in affected leaves from the different stages (S1, S2 and S3) compared to the HC (Table 1), and were the highest at S2. The number of proteins that increased in abundance was greater than the number of proteins that decreased in abundance. MFC-affected leaves at S2 presented higher number of proteins that increased in abundance (227 spots, Table 1) than the ones affected at S1 and S3 (142 and 77 spots, respectively).

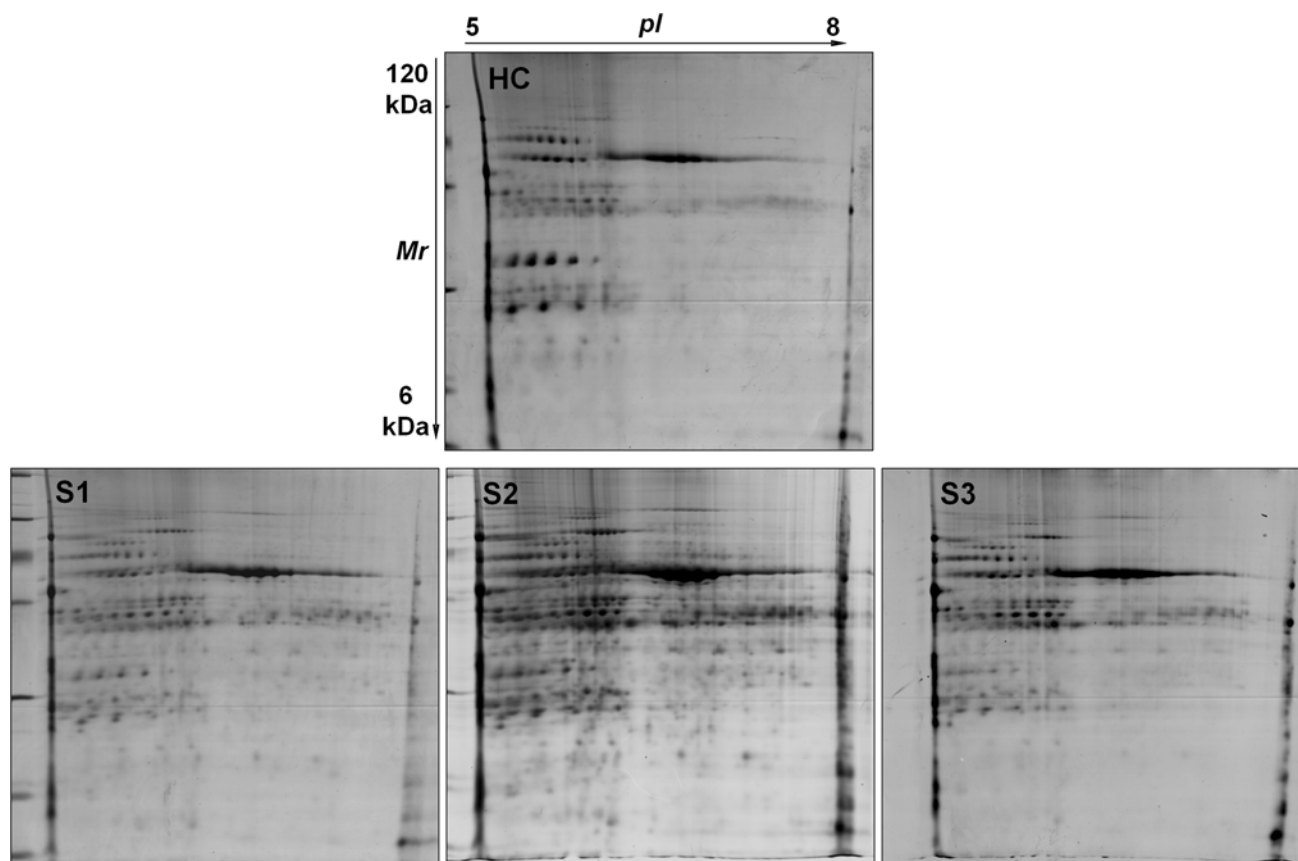


Fig. 2 Real 2-DE proteome map of healthy control (HC) and affected leaves taken from different disease stages (S1, S2 and S3). The relative M_r is given on the left, while the pI is given at the top. Five

hundred µg of proteins was separated in the first dimension on an immobilized, linear, 5–8 pH gradient and in the second dimension on a 12 % polyacrylamide–SDS gel

Table 1 Total number of spots and number of spots showing quantitative differences between healthy (HC) and MFC-affected leaves from different stages (S1, S2 and S3)

Stages	Protein content (µg/g DW)	Total number of spots	Up-accumulated	Down-accumulated
HC	253.86 ± 6	157.6 ± 2		
S1	284 ± 7.1	262.3 ± 2	142	22
S2	230.85 ± 9.3	342 ± 1	227	31
S3	235.88 ± 2.08	190.6 ± 1	77	34

Values are mean ± SD of three biological replicates. All the differences were statistically significant according to ANOVA test ($P \leq 0.01$). Up and down-accumulated proteins are calculated with respect to HC

Table 2 Principal components calculated from the 364 spots matched between samples

Eigenvalues			
PC	Value	Percent	Cumulative percent
1	28.47925	44.698	44.698
2	20.44358	32.086	76.784
3	14.79172	23.215	99.999
4	-0.00000	0	99.999

Statistical and expression cluster analyses

The whole protein data set was analyzed by PCA. The first three principal components accounted for 99.99 % of the biological variability of each spot dataset (Table 2). MFC-affected leaves from the three stages (S1, S2 and S3) and the HC are clearly separated (Fig. 3a). We found that the experimental conditions could be divided into three large clusters in a dendrogram, namely, cluster 5, cluster 6 and cluster 7 (Fig. 3b). This clustering indicated that affected leaves from stages S1 and S3 had a similar protein profile (clustering closest together; cluster 5). MFC-affected leaves from stages S2 were further away from the HC than those from S1 and S3.

Protein identification and differential expression analysis

Out of the 364 resolved spots, 297 were considered as being variable between samples after multivariate statistical analysis. One hundred and thirteen consistent proteins, present in three biological replicates, thus preventing the assignment of normalized volume values to missing spots for multivariate analysis (Valledor and Jorrín 2011), were subjected to MALDI-(TOF/TOF) mass spectrometry analysis, resulting in 58 confidence hits (Table 3). The major group of identified proteins corresponded to chloroplastic ones (60 %), these being involved in the photosynthesis electronic chain and ATP synthesis (31 %), carbohydrate metabolism and Calvin cycle [40 %, with 7 large ribulose-

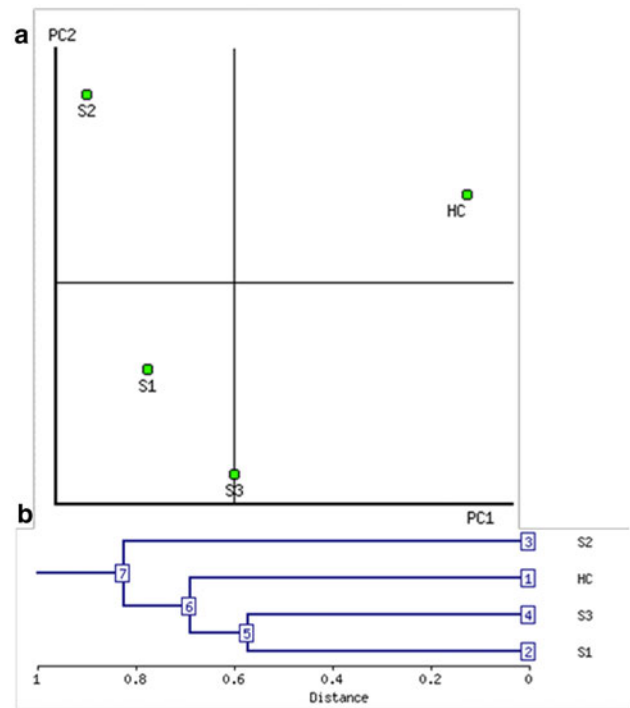


Fig. 3 Statistical protein expression cluster analysis of healthy control (HC) and affected leaves taken from different disease stages (S1, S2 and S3), using the ANOVA-based NIA array analysis tool (Sharov et al. 2005). **a** Two-dimensional plot showing separation of samples plotted in the first and the second component space by principal component analysis (PCA). **b** Dendrogram showing hierarchical clustering of samples. The expression clusters are numbered from 1 to 7

1.5-bisphosphate carboxylase/oxygenase large subunit (RubisCO)], and protein fate (14 %). Twelve percent of proteins were stress-related ones. Actin and porin have also been identified (Table 3).

In 46 % of total identified proteins, the same protein has been identified from different spots, and we can speculate that they were the products of isogenes or post-translational modifications (PTMs), variants of specific gene products differing in *pI* and/or *Mr*. Thus, the following proteins are examples of those with more than two spots: ATP synthase CF1 beta chain (found in 4 spots), oxygen-evolving system

Table 3 List of identified proteins

Spot number	Protein name (cellular localization) ^a	Organism/accession number ^b	<i>E</i> value ^c	Protein score/ protein score CI % ^d	MP	Theoretical <i>M_r</i> (kDa)/pI ^e	Experimental <i>M_r</i> (kDa)/pI ^f	Protein rate ^g		
								S1	S2	S3
<i>Metabolism</i>										
Photosynthesis and Calvin cycle										
4714	ATP1 gene product (mitochondrion)	<i>Phoenix dactylifera</i> gil372450225	5e–006	90/100	13	55.486/6.02	62.10/5.86	2.10	0.56	1.88
3502	ATP synthase beta subunit (chloroplastic)	<i>Phytelphas aequatorialis</i> gil13236810	4e–008	111/100	17	53.677/5.36	42.60/5.62	0.43	0.36	0.00
5712	ATP synthase beta subunit (chloroplastic)	<i>Elaeis oleifera</i> gil13236804	6.3e–033	359/100	21	53.819/5.29	59.2/6.04	∞	∞	∞
4603	ATP synthase CF1 beta chain (chloroplastic)	<i>Phoenix dactylifera</i> gil290790923	6.3e–016	189/100	26	53.847/5.29	57.64/5.94	∞	∞	∞
3601	ATP synthase CF1 beta chain (chloroplastic)	<i>Phoenix dactylifera</i> gil290790923	4e–037	401/100	32	53.847/5.29	57.51/5.67	0.59	0.76	0.48
2604	ATP synthase CF1 beta chain (chloroplastic)	<i>Phoenix dactylifera</i> gil290790923	1.2e–016	196/100	29	53.847/5.29	57.68/5.59	2.19	6.34	1.95
2203	ATP synthase CF1 beta chain (chloroplastic)	<i>Phoenix dactylifera</i> gil290790923	7.9e–018	208/100	29	53.847/5.29	32.83/5.43	∞	∞	∞
3715	V-type proton ATPase catalytic subunit A (vacuole)	<i>Arabidopsis thaliana</i> gil3334404	1.5e–009	127/100	15	69.111/5.11	84.88/5.80	∞	∞	∞
3716	V-type proton ATPase catalytic subunit A (vacuole)	<i>Arabidopsis thaliana</i> gil3334404	0.0051	62/95.81	4	69.111/5.11	85.11/5.74	∞	∞	∞
2213	Oxygen-evolving system of photosystem II = OEC 33 kDa subunit. Manganese-stabilizing protein 2 (chloroplastic)	<i>Arabidopsis thaliana</i> gil11134146	2.3e–010	135/100	8	35.226/5.92	33.12/5.53	2.18	1.03	1.31
2205	Oxygen-evolving system of photosystem II = OEC 33 kDa subunit. Manganese-stabilizing protein 2 (chloroplastic)	<i>Arabidopsis thaliana</i> gil11134146	1.5e–013	167/100	10	35.226/5.92	33.49/5.44	∞	∞	∞
2211	Oxygen-evolving system of photosystem II = OEC 33 kDa subunit. Manganese-stabilizing protein 2 (chloroplastic)	<i>Arabidopsis thaliana</i> gil11134146	5.9e–010	131/100	8	35.226/5.92	33.21/5.56	0.48	0.42	0.53
4201	Oxygen-evolving system of photosystem II = OEC 33 kDa subunit. Manganese-stabilizing protein 2 (chloroplastic)	<i>Arabidopsis thaliana</i> gil11134146	3.7e–013	163/100	8	35.226/5.92	33.61/5.85	∞	∞	∞
4206	Oxygen-evolving system of photosystem II = OEC 33 kDa subunit. Manganese-stabilizing protein 2 (chloroplastic)	<i>Arabidopsis thaliana</i> gil11134146	2.3e–016	195/100	10	35.226/5.92	33.14/5.84	∞	∞	∞

Table 3 continued

Spot number	Protein name (cellular localization) ^a	Organism/accession number ^b	E value ^c	Protein score/protein score CI % ^d	MP	Theoretical M_r (kDa)/pI ^e	Experimental M_r (kDa)/pI ^f	Protein rate ^g		
								S1	S2	S3
3204	Oxygen-evolving system of photosystem II = OEC 33 kDa subunit. Manganese-stabilizing protein 1 (chloroplastic)	<i>Arabidopsis thaliana</i> gil15240013	2.4e-006	104/100	12	35.349/5.55	33.30/5.69	0.48	0.95	0.54
6613	Ribulose-1,5-bisphosphate carboxylase/oxygenase large subunit (plastid)	<i>Dictyosperma album</i> gil90968352	9.9e-015	177/100	15	48.742/6.23	53.81/6.48	∞	∞	∞
5209	Ribulose-1,5-bisphosphate carboxylase/oxygenase large subunit (plastid)	<i>Dryophloeus subditichus</i> gil552532	5e-008	110/100	10	52.710/6.33	30.02/6.11	∞	∞	∞
6102	Ribulose-1,5-bisphosphate carboxylase/oxygenase large subunit (plastid)	<i>Iriartella stenocarpa</i> gil113207510	0.00015	75/99.98	13	49.066/6.23	28.70/6.49	0.006	0.7	0.03
6106	Ribulose-1,5-bisphosphate carboxylase/oxygenase large subunit (plastid)	<i>Prestoea pubens</i> gil90968302	8.4e-005	78/99.99	13	48.776/6.23	27.89/6.52	∞	∞	∞
6101	Ribulose-1,5-bisphosphate carboxylase/oxygenase large subunit (plastid)	<i>Caryota mitis</i> gil1370005	0.02	54/98.02	10	52.526/6.33	28.85/6.61	0.07	0.50	0.00
7311	Ribulose-1,5-bisphosphate carboxylase/oxygenase large subunit (plastid)	<i>Dictyosperma album</i> gil90968352	1.2e-018	216/100	19	48.742/6.23	33.13/6.85	∞	∞	∞
8310	Ribulose-1,5-bisphosphate carboxylase/oxygenase large subunit (plastid)	<i>Phoenix dactylifera</i> gil90968260	1.6e-026	295/100	20	48.783/6.34	32.93/7.25	∞	∞	∞
7313	Ferredoxin—NADP reductase, leaf isozyme 1 (chloroplastic)	<i>Arabidopsis thaliana</i> gil75171342	0.0002	76/99.98	2	40.643/8.32	37.14/6.62	∞	∞	∞
7312	Ferredoxin—NADP reductase, leaf isozyme 1 (chloroplastic)	<i>Arabidopsis thaliana</i> gil75171342	9.8e-005	79/99.99	6	40.643/8.32	36.37/6.96	∞	∞	∞
6105	FQR1 (flavodoxin-like quinone reductase 1) (vacuolar membrane)	<i>Arabidopsis thaliana</i> gil15239652	9.6e-014	178/100	9	21.782/5.96	27.21/6.51	∞	∞	∞
<i>Carbohydrate metabolism</i>										
3710	Enolase	<i>Elaeis guineensis</i> gil192910834	1.6e-010	135/100	11	48.127/5.98	62.25/5.76	0.00	0.00	0.00
3711	Enolase	<i>Elaeis guineensis</i> gil192910834	2.5e-034	373/100	17	48.127/5.98	62.23/5.68	∞	∞	∞
3707	Enolase	<i>Elaeis guineensis</i> gil192910834	4e-016	191/100	13	48.127/5.98	67.49/5.81	0.28	0.14	0.11
3505	Phosphoglycerate kinase (chloroplastic)	<i>Arabidopsis thaliana</i> gil332278232	5.9e-012	151/100	8	50.008/6.23	45.24/5.75	0.63	0.00	0.00

Table 3 continued

Spot number	Protein name (cellular localization) ^a	Organism/accession number ^b	E value ^c	Protein score/protein score CI % ^d	MP	Theoretical M_r (kDa)/pI ^e	Experimental M_r (kDa)/pI ^f	Protein rate ^g		
								S1	S2	S3
7520	Glyceraldehyde 3-phosphate dehydrogenase	<i>Elaeis guineensis</i> gil82400215	5e-015	180/100	9	32.250/7.05	41.25/7.05	∞	∞	∞
7608	Glyceraldehyde 3-phosphate dehydrogenase	<i>Elaeis guineensis</i> gil82400215	0.015	55/99.91	4	32.250/7.05	43.57/6.96	∞	∞	∞
7609	Glyceraldehyde 3-phosphate dehydrogenase	<i>Elaeis guineensis</i> gil82400215	5.3e-007	100/100	5	32.250/7.05	43.49/6.87	∞	∞	∞
7409	Malate dehydrogenase (cytoplasmic)	<i>Arabidopsis thaliana</i> gil11133446	2.5e-006	95/100	9	35.995/6.33	38.70/7.12	∞	∞	∞
5206	Triose phosphate isomerase (cytosolic isoform)	<i>Elaeis guineensis</i> gil192910674	2e-015	184/100	8	27.476/5.87	30.56/6.00	6.12	3.92	4.32
5208	Triosephosphate isomerase (cytosolic)	<i>Arabidopsis thaliana</i> gil15233272	0.0082	69/100	4	27.380/5.39	30.36/6.04	∞	∞	∞
4109	Putative soluble inorganic pyrophosphatase	<i>Elaeis guineensis</i> gil374255979	5e-010	130/100	6	19.772/5.41	29.18/5.94	∞	∞	∞
6609	Hydroxypyruvate reductase (chloroplastic)	<i>Arabidopsis thaliana</i> gil15220620	0.012	67/100	15	42.449/6.68	44.61/6.66	∞	∞	∞
1513	Sedoheptulose-1,7-bisphosphatase (chloroplastic)	<i>Spinacia oleracea</i> gil3914940	0.00012	67/100	2	42.568/5.87	42.10/5.42	∞	∞	∞
5106	D-ribulose-5-phosphate-3-epimerase (chloroplastic)	<i>Arabidopsis thaliana</i> gil15240250	7.6e-024	279/100	6	30.275/8.24	28.54/6.10	∞	∞	∞
<i>Amino acid biosynthesis</i>										
2509	Putative glutamine synthetase cytosolic isozyme1 (cytosolic)	<i>Elaeis guineensis</i> gil35344112	7.9e-015	178/100	5	11.63/9.64	43.21/5.54	∞	∞	∞
7401	Putative glutamine synthetase cytosolic isozyme1 (cytosolic)	<i>Elaeis guineensis</i> gil35344112	0.004	61/100	2	11.63/9.64	40.64/6.93	∞	∞	∞
<i>Protein fate (synthesis and turnover)</i>										
3801	ATP-dependent Clp protease. Casein lytic proteinase C2 (chloroplastic)	<i>Arabidopsis thaliana</i> gil186510816	1.9e-008	125/100	25	105.90/6.06	103.99/5.82	∞	∞	∞
3802	ATP-dependent Clp protease. Casein lytic proteinase C2 (chloroplastic)	<i>Arabidopsis thaliana</i> gil186510816	1.9e-012	165/100	28	105.90/6.06	105.51/5.78	∞	∞	∞
4802	ATP-dependent Clp protease. Casein lytic proteinase C2 (chloroplastic)	<i>Arabidopsis thaliana</i> gil186510816	1.2e-017	217/100	33	105.90/6.06	101.15/5.93	∞	∞	∞

Table 3 continued

Spot number	Protein name (cellular localization) ^a	Organism/accession number ^b	E value ^c	Protein score/ protein score CI % ^d	MP	Theoretical M_r (kDa)/pI ^e	Experimental M_r (kDa)/pI ^f	Protein rate ^g		
								S1	S2	S3
5801	ATP-dependent Clp protease. Casein lytic proteinase C2 (chloroplastic)	<i>Arabidopsis thaliana</i> gil186510816	0.015	66/98.55	12	105.93/6.06	100.66/6.01	0.41	0.34	0.08
4803	ATP-dependent Clp protease. Casein lytic proteinase C2 (chloroplastic)	<i>Arabidopsis thaliana</i> gil7576225	3.8e-014	182/100	31	105.93/6.06	102.38/5.89	∞	∞	∞
4801	ATP-dependent Clp protease. Casein lytic proteinase C1 (chloroplastic)	<i>Arabidopsis thaliana</i> gil18423214	7.6e-008	119/100	23	103.61/6.36	101.15/5.97	∞	∞	∞
3206	Proteasome subunit alpha type-4	<i>Arabidopsis thaliana</i> gil12643237	3.0 × 10 ⁻¹¹	160/100	4	27.47/6.60	30.05/5.75	0.53	0.33	0.23
6103	Proteasome subunit beta type-1	<i>Arabidopsis thaliana</i> gil15232965	6.9e-005	89/99.99	6	24.85/6.95	28.44/6.35	∞	∞	∞
<i>Stress-related proteins</i>										
4202	Ascorbate peroxidase (cytosolic)	<i>Elaeis guineensis</i> gil192912966	6.3e-033	359/100	16	27.54/5.42	30.00/5.89	∞	∞	∞
7407	Peroxisome type ascorbate peroxidase	<i>Elaeis guineensis</i> gil192910808	0.0038	61/99.62	5	31.96/6.77	41.25/7.01	∞	∞	∞
5207	Putative ascorbate peroxidase protein (cytosolic)	<i>Elaeis guineensis</i> gil374256065	0.009	57/99.09	10	27.56/5.51	30.76/6.00	∞	∞	∞
3002	Peroxiredoxin	<i>Elaeis guineensis</i> gil192910922	9.9e-021	237/100	4	17.35/5.18	20.04/5.65	0.48	0.09	0.52
2005	Peroxiredoxin	<i>Elaeis guineensis</i> gil192910922	9.9e-014	167/100	3	17.35/5.18	19.87/5.45	∞	∞	∞
3712	Heat shock 70 kDa protein 7 (chloroplastic)	<i>Arabidopsis thaliana</i> gil15240578	0.012	67/98.84	13	77.06/5.17	89.95/5.79	∞	∞	∞
4713	Chaperonin 60 subunit beta 1 (chloroplastic)	<i>Arabidopsis thaliana</i> gil27735252	0.022	55/97.8	11	64.16/6.21	61.33/5.97	∞	∞	∞
<i>Cytoskeleton</i>										
2607	Actin (cytoplasm)	<i>Elaeis guineensis</i> gil48527433	2e-019	224/100	14	41.94/5.24	46.49/5.56	0.31	0.60	0.47

Table 3 continued

Spot number	Protein name (cellular localization) ^a	Organism/accession number ^b	E value ^c	Protein score/protein score CI % ^d	MP	Theoretical M_r (kDa)/ pI ^e	Experimental M_r (kDa)/ pI ^f	Protein rate ^g		
								S1	S2	S3
7317	Mitochondrial outer membrane protein porin of 34 kDa	<i>Solanum tuberosum</i> gil1172555	1.0×10^{-2}	93/98.91	1	29.57/8.68	32.89/6.99	∞	∞	∞

The proteins are listed under broad functional categories

MP matched peptides

^a NCBI database name and cellular localization of protein

^b NCBI database organism and accession numbers of protein

^c Expect value that describes the number of hits one can expect to see by chance

^d MOWSE score probability (protein score) for the entire protein and for ions complemented by the percentage of the confidence index (CI). Protein scores >49 are significant ($P < 0.05$)

^e Theoretical molecular weight (kDa) and pI annotated in the NCBI database

^f Experimental molecular weight (kDa) and pI

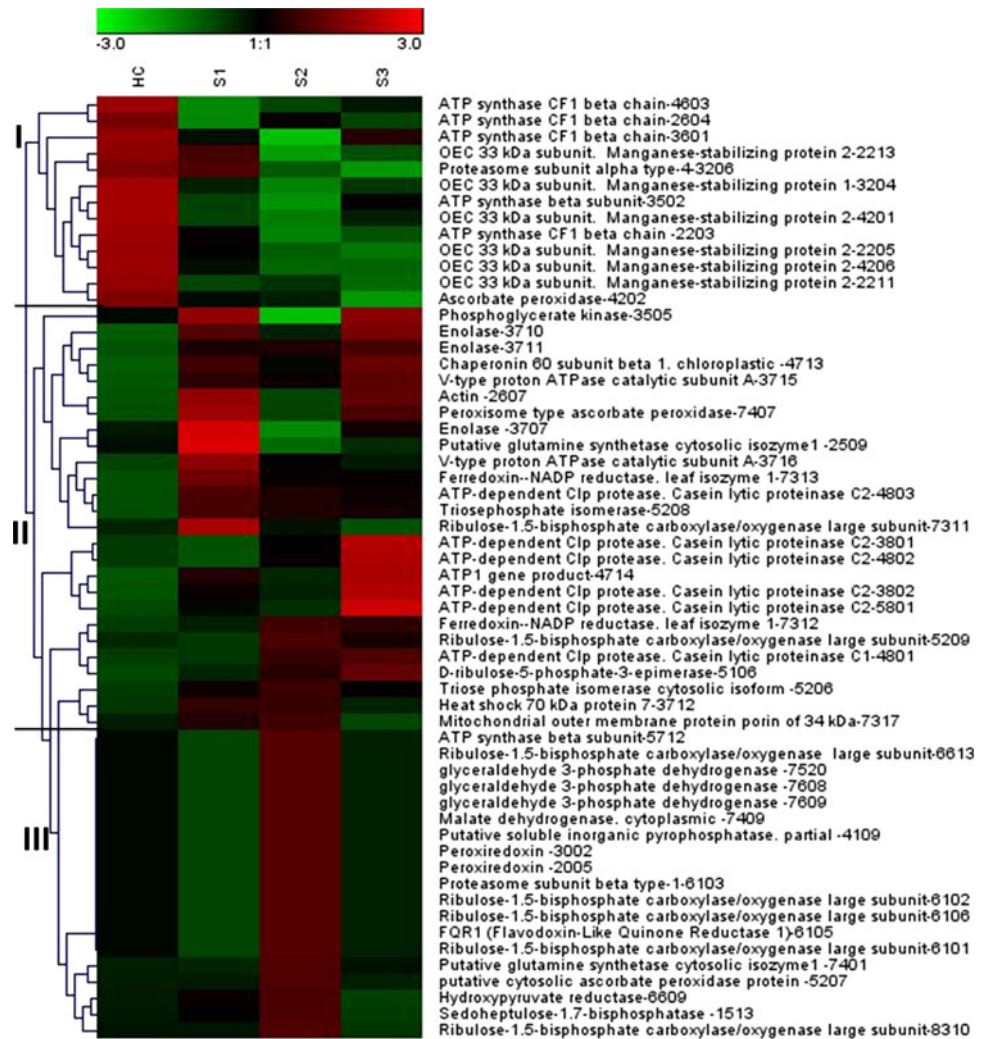
^g The rate was calculated by dividing the mean values of the proteins from affected palm leaves with respect to control (HC). ∞, the spot was detected in the affected palm leaves instead of the HC. 0, the spot was detected in the HC instead of the inoculated seedlings

(OEC) of photosystem II 33 kDa subunit or manganese-stabilizing proteins (MSP-33 kDa; found in 6 spots), RubisCO (4), enolase (3), ATP-dependent Clp protease (6). For those spots with significantly lower experimental values than theoretical M_r , protein degradation can be proposed (RubisCO; spots 6102, 6106, 6101, 7311 and 8310), and for those with higher experimental M_r (putative glutamine synthetase cytosolic isozyme; spots 2509 and 7401), PTMs such as ubiquitination or aggregation processes, but these must be experimentally validated.

The different expression dynamics of each identified protein could be distinguished in the heat map allowing a definition of three expression groups (Fig. 4). The first one showed high protein abundance throughout the HC (Fig. 4, in red) and a low one for the affected leaves from three stages (in green), including proteins of the photosynthesis electronic chain and ATP synthesis. The second group showed an opposite trend to the first one, and the third group showed high expression protein abundance only at the S2 stage. The second and third groups resemble the proteases and proteins from Calvin cycle and carbohydrate metabolism (Fig. 4).

Proteins belonging to the photosynthesis electronic chain and ATP synthesis (ATP synthase; spots 3502, 4603, 3601, 2604 and 2203, and MSP-33 kDa subunit proteins; spots 2213, 2205, 2211, 4206 and 3204) showed a decrease in affected leaves from three disease stages (Figs. 4, 5). On the contrary, ATP-dependent Clp protease proteins (spots: 3801, 3802, 4802, 5801, 4803 and 4801) increased in abundance in affected leaflets, these being more abundant at S3 stage (spots: 3801, 3802, 4802 and 5801). For those RubisCO proteins (spots: 6613, 5209, 6102, 6106, 6101, 7311 and 8310) identified in the present study, 87.5 % of which present lower (0.5 fold) experimental values than theoretical M_r , protein degradation processes can be proposed. RubisCO proteins increased in the affected leaflets (Figs. 4, 5). MFC led to the decrease in MSP-33 kDa subunit proteins (spots 2205, 2211, 2213, 3204, 4201 and 4206) and ATP synthase beta subunit (spots 2203, 2604, 3502, 3601 and 4603) in date palm leaves from three characteristic stages. Chloroplastic (phosphoglycerate kinase, 3505; sedoheptulose-1,7-bisphosphatase, 1513 and D-ribulose-5-phosphate-3-epimerase, 5106), and cytosolic (enolase, 3710 and 3711; triosephosphate isomerase, 5208 and 5206; and glyceraldehyde 3-phosphate dehydrogenase, 7520, 7608, 7609; Figs. 4, 5) metabolic enzymes increased in the affected leaflets. Two chloroplastic proteins have been identified as stress-related proteins in our work in response to MFC; the heat shock 70 kDa (Hsp; spot 3712) and chaperonin 60 subunit beta 1 (4713) which increased in the affected leaves taken from stage S2 and S3, respectively (Figs. 4, 5). Other stress-related proteins identified as peroxiredoxin (spots 2005 and 3002) increased only at the

Fig. 4 Hierarchical clustering of the differentially regulated proteins identified in this study. A heat map representation shows the protein value according to the level of normalized experiments which are indicated from -3 (minimum positive expression; green color) to 3 (maximum positive expression; red color); black indicates zero expression. Leaves were sampled from both healthy control (HC) and affected leaves taken from different disease stages (S1, S2 and S3)



S2 stage. Protein (spot 2607) identified as actin increased at stages S1 and S3; however, it was not detected in affected palm leaf from stage S2. Finally, we have observed an increase in mitochondrial outer membrane protein porin of 34 kDa from affected leaflets at S2, and this was not observed at S3.

Discussion

In palm trees with early MFC symptoms (stage S1), some fronds show chlorosis and have a dull, olive green color. At this disease stage, we cannot discriminate exactly the HC from the affected tree visually (for that reason HC was taken from a location where MFC symptoms have never been detected), however, at S2 and S3 stages, the presence of the MFC disease is clearly seen. Healthy and affected leaves result from offshoot propagation also named vegetative propagation. The offshoots develop from axillary

buds on the trunk of the mother plant and consequently conserve the same genetic information. Therefore, all the protein variations observed may result only from the disease’s progression.

The different protein samples were separated by 2-DE with IEF carried out in the 5–8 pH range, taking into consideration that the use of the 3–10 pH range in date palm leaves tissues (Gómez-Vidal et al. 2009), resulted in obtaining of protein spots concentrated in 5–8 pH region. Similar results were also observed for somatic and zygotic date palm embryos Sghaier-Hammami et al. (2009a, b, 2010). 2-DE protein profile of the HC seems to be poorer in protein spots than MFC-affected leaves at S1, S2 and S3 stages, which may be due to the fact that it is easier to extract proteins from leaves affected by MFC, compared to the fibrous HC counterparts. Moreover, MFC-affected leaves at S2 presented higher number of proteins that increased in abundance than the ones affected at S1 and S3. Indeed, it is during this stage that several metabolic and

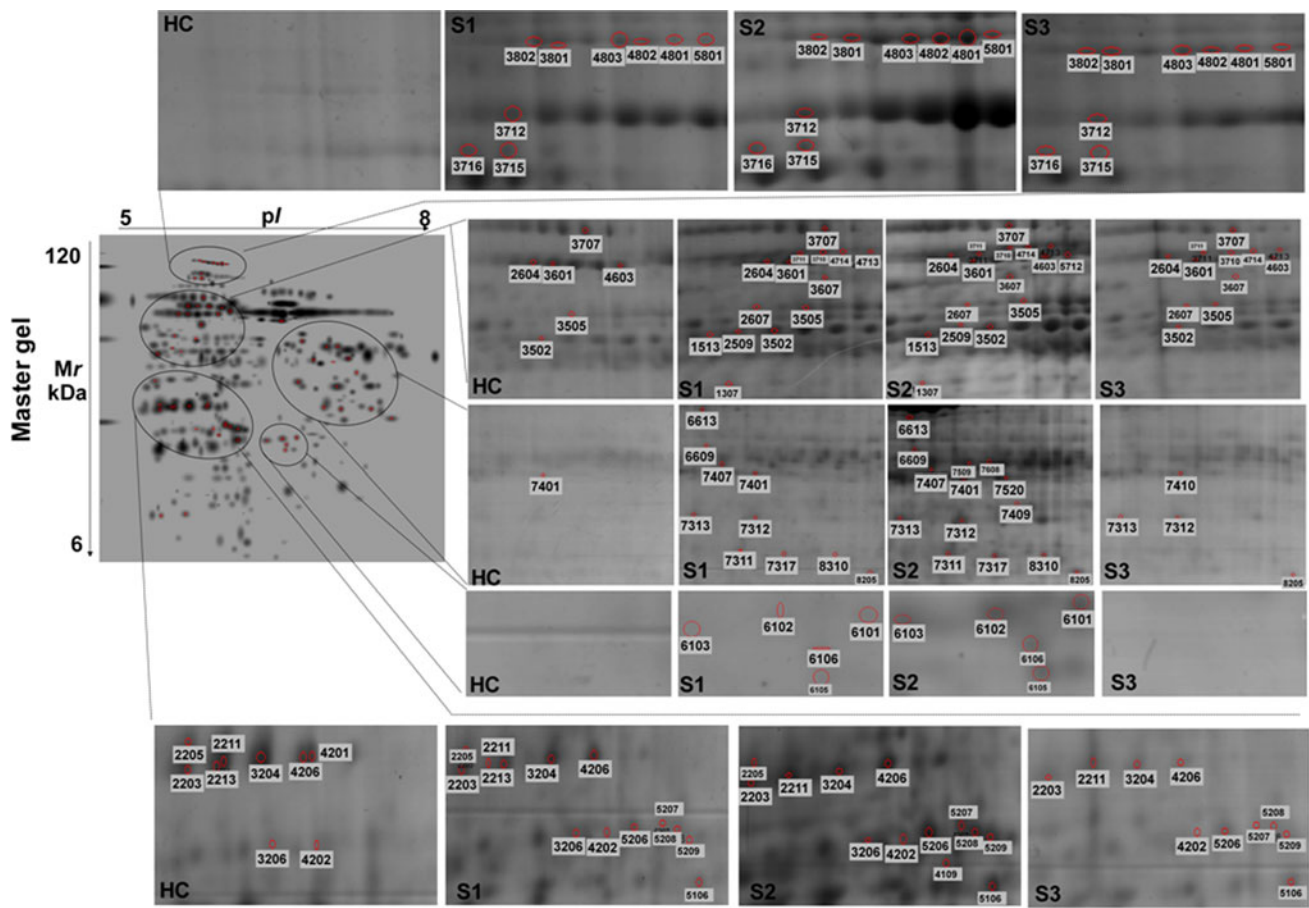


Fig. 5 Representative 2-DE master gel of healthy control (HC) and affected leaves taken from different disease stages (S1, S2 and S3). Gel areas are magnified to visualize differential spots. Only identified protein spots are shown and numbered

phenotypic changes take place in the plant and leaves (Saadi et al. 2006).

Comparatively, a 2-DE protein map (with a 3–10 pH range) from similar proteomics studies realized on affected leaves at S2 stage (Marqués et al. 2011) showed that the leaflets of MFC-affected and HC palms do not contain striking qualitative differences either in the number or in the amount of the most abundant protein species detected by colloidal Coomassie blue staining (Marqués et al. 2011). This could be explained by the use of different extraction methods and different ranges of pH. In a proteomics study, the protein extraction protocol greatly affects the quality of the extract and every modification in sample preparation generates variability for both protein identification and quantitation (Maldonado et al. 2008; Zhang et al. 2011; Sghaier-Hammami et al. 2012). It is important to emphasize that the TCA–acetone–phenol method was previously successfully used for date palm tissues such as leaves Gómez-Vidal et al. (2009) and embryos (Sghaier-Hammami et al. 2009a, b, 2010).

Nowadays, the employment of statistics analyses is being widely used, these being the basis of system biology because of their capacity to interrelate different variables and they can sometimes be helpful in selecting candidate spots (Kreutz and Timmers 2008). PCA is a strong approach and is used to obtain an overview of the main variation and any interrelations between spots in the protein patterns (Valledor and Jorrín 2011). Heat map analysis was considered as the most accurate procedure for proteomics data (Meunier et al. 2007). Following the use of the PCA and heat map analyses, it is clear that the remaining spots were different enough to differentiate MFC-affected leaves from the healthy ones, and that the greatest change in the 2-DE protein profile occurred during the S2 disease stage.

The proteomic analysis carried out in the present work has shown that among the 58 successfully identified proteins, 54 have not been reported previously in similar proteomics studies of the MFC-date palm (Marqués et al. 2011). Half of the total identified proteins, may result from

a product of isogenes or post-translational modifications (PTMs), variants of specific gene products differing in *pI* and/or *Mr*. The presence of protein isoforms with different expression patterns has been reported previously in date palm (Sghaier-Hammami et al. 2009a, b, 2010; Marqués et al. 2011) and in other species like *Arabidopsis* (Sghaier-Hammami et al. 2012).

Differential identified proteins belonged to different groups including those of photosynthesis and Calvin cycle, carbohydrate metabolism, amino acid biosynthesis, protein fate (synthesis and turnover), stress-related proteins and cytoskeleton. Seven RubisCO protein species have been identified in the present work, six of which seem to be a product of protein degradation processes. It has been demonstrated that RubisCO can be degraded in intact pea chloroplasts (Mitsuhashi et al. 1992). During senescence, RubisCO accounts for about 90 % of the degraded proteins (Miller and Huffaker 1985). Under abiotic stress, a rapid net degradation of RubisCO fragments of the large subunit may become detectable on immunoblots. However, during natural senescence, often only the bands representing the intact large and small subunits (but no fragments) are visible on stained gels or immunoblots (Feller et al. 2008). A clear degradation of RubisCO and other chloroplast proteins can be observed during initiated leaf senescence as well as during or after abiotic stress phases (Crafts-Brandner and Egli 1987; Crafts-Brandner et al. 1998; Demirevska-Kepova et al. 2004; Feller et al. 2008). The observed leaf chlorosis during the S2 disease stage may be in relation with the RubisCO degradation. The degradation of RubisCO reinforces the hypothesis that MFC-affected date palm leaves are caused by an abiotic stress (Mn deficiency).

The increase in RubisCO proteins, as well as the increase in ATP-dependent chloroplastic proteases is observed in MFC-affected leaflets. Chloroplast proteases participate in chloroplast biogenesis during adaptation to changing environmental conditions through degradation of certain proteins, and maintenance of protein quality through degradation of unassembled or damaged proteins (Adam et al. 2006). Roberts et al. (2003) reported the role of serine protease activity in senescing wheat leaves for which RubisCO was a target protein. The ATP-dependent chloroplast proteases identified in our study are classified as serine endopeptidases (http://www.genome.jp/dbget-bin/www_bget?ec:3.4.21.92), and may enhance photoinhibition (<http://www.uniprot.org/uniprot/Q9SXJ7>). The increase in ATP-dependent clp proteases may also play an important role for the photosystem complexes, since the formation and maintenance of a functional thylakoid electron transport chain require various protease activities, operating in parallel, as well as in series (Dominic et al. 2011). Our previous results (Saidi et al. 2012) showed that MFC led to a decrease in

photosynthetic activity and the diminution of chlorophyll content by enzymatic degradation via chlorophyllase. Consequently, we can consider RubisCO and ATP-dependent clp proteases as MFC proteins biomarkers.

MFC led to the decrease in MSP-33 kDa subunit proteins and ATP synthase beta subunit in affected leaflets from three characteristic stages. Mn is a key element in photosynthetic water reduction and oxygen evolution. It is also a constituent of respiratory enzymes (Adriano 2001). Mn deficiency in green plants is known to affect preferentially the activity of the OEC (Homann 1967). In plants, the integrity and optimal function of the OEC depend on the presence of extrinsic MSP-33 kDa subunit proteins, which play a central role in maintaining the integrity and activity of the manganese cluster (Seidler 1996). The decrease in the ATP synthase, MSP-33 kDa subunit proteins and the luminal OEC proteins (PSBO2, PSB, PSBP and PSBO1) in the study of Marqués et al. (2011) reinforce the hypothesis of the relation between the MFC and Mn deficiency. We can consider the decrease in the MSP-33 kDa subunit proteins and ATP synthase proteins as biomarkers of the Mn deficiency in MFC-affected date palm leaves.

Both the chloroplastic and cytosolic metabolic enzyme increased in the affected leaflets. Similarly, it has been demonstrated that chloroplastic transketolase, triosephosphate isomerase and cytoplasmic malate dehydrogenase increased in diseased leaflets (Marqués et al. 2011).

The typical stress response of a plant is the induction of the stress-related proteins including the chloroplastic Hsp70 kDa and chaperonin 60 subunit beta 1 proteins. Also, our transcriptomic analysis showed that a cDNA fragment related to Hsp70 was up-regulated in affected leaves (Saidi et al. 2010). Hsp may play a role in cross-talk with other mechanisms and function synergistically with other components to decrease cell damage (Hartl 1996; Bukau and Horwich 1998). The Chaperonin 60 subunit beta 1 showed itself to be implicated in cell death and systemic acquired resistance (<http://www.uniprot.org/uniprot/P21240>) and to play a role in acclimating photosynthesis to heat stress, possibly by protecting RubisCO activase from thermal denaturation (Salvucci 2008). Other stress-related proteins identified such as peroxiredoxin increased only at the S2 stage. Plant 2-Cys peroxiredoxins are post-translationally targeted to chloroplasts, where they protect the photosynthetic membrane against photooxidative damage (Baier and Dietz 1997, 1999). At a transcriptomic level, our group has found that manganese deficiency in the BLD affected date palm induces an oxidative stress especially at S2 stage (Saidi et al. 2012).

Of interest is the increase of actin, which has recently been related to programmed cell death (PCD). Recent live cell imaging techniques have revealed dynamic features

and significant roles of cytoskeletons during defense responses and PCD (Higaki et al. 2011). One unexpected result is that we did not detect this protein in the affected palm leaf from stage S2; however, it increased at stages S1 and S3.

Finally, we have observed an increase in mitochondrial outer membrane protein porin of 34 kDa from affected leaflets at S2, and this was not observed at S3. Similarly, this protein was also seen to be increased at S2 in the previous study by Marqués et al. (2011). The porin proteins form a channel through the mitochondrial outer membrane that allows the diffusion of small hydrophilic molecules (<http://www.uniprot.org/uniprot/Q6K548>). The absence of porin at S3 may be explained by the fact that symptoms extend to the entire plant that finally dies.

In conclusion, the present proteomics work permits the dissection of the MFC disease from the early to the last disease steps (death of the palm tree). Changes in the 2-DE protein profile start at early disease stage (S1), in which we have especially observed a decrease in MSP-33 kDa subunit proteins. From the S2 stage, when leaflets became chlorotic, we have observed degradation of the RubisCO proteins. This is not only specific to Mn deficiency, but confirms that MFC is an abiotic stress. From this stage, MSP-33 kDa subunit proteins continue to decrease together with ATP synthase. One unexpected result is the increase of the actin at the S3 stage, in which leaflets break when flexed and squeezed, but it may be a signal of the PCD. At this stage, MSP-33 kDa subunit proteins also decrease and we have observed an extensive increase of the ATP-dependent clp proteases. All the observed protein changes, related to MFC disease, may also be related to the other stress response. However, the decrease in the MSP-33 kDa subunit proteins is closely related to the Mn deficiency. Therefore, MSP-33 kDa subunit proteins can be considered as a MFC biomarker, specifically at an early MFC disease stage, at which symptoms may not reflect the disease's intensity. As perspective to this work, it would be of interest to seek an antibody against this protein, and with an ELISA test or immunoblot, we could predict the presence of the MFC disease early. Then, the discrimination of the disease could be avoided (by eliminating the diseased tree), since its progression is apparently transmitted from an affected tree to neighboring trees.

Acknowledgments This work is supported by “le Ministère de l'Enseignement Supérieur, de la Recherche Scientifique et de la Technologie” of Tunisia. We gratefully acknowledge support from Dr. Lola Gutierrez Blázquez (Proteomics Service, University of Madrid) for mass spectrometry facilities and technical assistance. Authors thank Dr. Lyudmila Simova from Institute of Plant Physiology, Bulgarian Academy of Sciences for critical review of the manuscript, and Dr. Anne-Lise Haenni from Institut Jacques Monod Paris for her kind help in correcting the English.

References

- Adam Z, Rudella A, van Wijk KJ (2006) Recent advances in the study of Clp, FtsH and other proteases located in chloroplasts. *Curr Opin Plant Biol* 9:234–240
- Adriano DC (2001) Manganese. Trace elements in terrestrial environments. Springer, Berlin, pp 547–585
- Baier M, Dietz KJ (1997) The plant 2-Cys peroxiredoxin BAS1 is a nuclear-encoded chloroplast protein: its expressional regulation, phylogenetic origin, and implications for its specific physiological function in plants. *Plant J* 12:179–190
- Baier M, Dietz KJ (1999) Protective function of chloroplast 2-cysteine peroxiredoxin in photosynthesis. Evidence from transgenic Arabidopsis. *Plant Physiol* 119:1407–1414
- Bradford M (1976) A Rapid and sensitive method for the quantitation of microgram quantities of protein utilizing the principle of protein–dye binding. *Anal Biochem* 72:248–254
- Brumbarova T, Matros A, Mock H-P, Bauer P (2008) A proteomic study showing differential regulation of stress, redox regulation and peroxidase proteins by iron supply and the transcription factor FER. *Plant J* 54:321–334
- Bukau B, Horwich AL (1998) The Hsp70 and Hsp60 chaperone machines. *Cell* 92:351–366
- Castillejo MA, Curto M, Fondevilla S, Rubiales D, Jorrín JV (2010a) Two-dimensional electrophoresis based proteomic analysis of the pea (*Pisum sativum*) in response to *Mycosphaerella pinodes*. *J Agric Food Chem* 58:12822–12832
- Castillejo MA, Kirchev H, Jorrín JV (2010b) Differences in the Triticale (X *Triticosecale Wittmack*) flag leaf 2-DE protein profile between varieties and nitrogen fertilization levels. *J Agric Food Chem* 58:5698–5707
- Chich JF, David O, Villers F, Schaeffer B, Lutowski D, Huet S (2007) Statistics for proteomics: experimental design and 2-DE differential analysis. *J Chromatogr B* 849:261–272
- Crafts-Brandner SJ, Egli DB (1987) Sink removal and leaf senescence in soybean: cultivar effects. *Plant Physiol* 85:662–666
- Crafts-Brandner SJ, Hölzer R, Feller U (1998) Influence of nitrogen deficiency on senescence and the amounts of RNA and proteins in wheat leaves. *Physiol Plant* 102:192–200
- Demirevska-Kepova K, Simova-Stoilova L, Stoyanova Z, Hölzer R, Feller U (2004) Biochemical changes in barley plants after excessive supply of copper and manganese. *Environ Exp Bot* 52:253–266
- Dominic BP, Olinares PDB, Kim J, van Wijk KJ (2011) The Clp protease system; a central component of the chloroplast protease network. *Biochim Biophys Acta* 1807:999–1011
- Eisen MB, Spellman PT, Brown PO, Botstein D (1998) Cluster analysis and display of genome-wide expression patterns. *Proc Natl Acad Sci USA* 95:14863–14868
- Feller U, Anders I, Mae T (2008) Rubiscolytics: fate of Rubisco after its enzymatic function in a cell is terminated. *J Exp Bot* 59:1615–1624
- Gómez-Vidal S, Salinas J, Tena M, Lopez-Llorca LV (2009) Proteomic analysis of date palm (*Phoenix dactylifera* L.) responses to endophytic colonization by entomopathogenic fungi. *Electrophoresis* 30:2996–3005
- Hartl FU (1996) Molecular chaperones in cellular protein folding. *Nature* 381:571–580
- Higaki T, Kurusu T, Hasezawa S, Kuchitsu K (2011) Dynamic intracellular reorganization of cytoskeletons and the vacuole in defense responses and hypersensitive cell death in plants. *J Plant Res* doi:10.1007/s10265-10011-10408-z
- Homann PH (1967) Studies on the manganese of the chloroplast. *Plant Physiol* 42:997–1007

- Kreutz C, Timmers J (2008) Systems biology: experimental design. *FEBS J* 276:923–942
- Maldonado AM, Echevarría-Zomeño S, Jean-Baptiste S, Hernández M, Jorrín-Novo JV (2008) Evaluation of three different protocols of protein extraction for *Arabidopsis thaliana* leaf proteome analysis by two-dimensional electrophoresis. *J Proteomics* 71:461–472
- Marqués J, Fadda ZG, Duran-Vila N, Flores R, Bové JM, Daròs JA (2008) A set of novel RNAs transcribed from the chloroplast genome accumulates in date palm leaflets affected by brittle leaf disease. *Phytopathology* 98:337–344
- Marqués J, Duran-Vila N, Daròs JA (2011) The Mn-binding proteins of the photosystem II oxygen-evolving complex are decreased in date palms affected by brittle leaf disease. *Plant Physiol Biochem* 49:388–394
- Meunier B, Dumas E, Picc I, Béchet D, Hébraud M, Hocquette JF (2007) Assessment of hierarchical clustering methodologies for proteomic data mining. *J Proteome Res* 6:358–366
- Miller B, Huffaker LRC (1985) Differential induction of endoproteases during senescence of attached and detached barley leaves. *Plant Physiol* 78:442–446
- Mitsuhashi W, Crafts-Brandne SJ, Feller U (1992) Ribulose-1,5-bisphosphate carboxylase/oxygenase degradation in isolated pea chloroplasts incubated in the light or in the dark. *J Plant Physiol* 139:653–658
- Namsi A, Montarone M, Serra P, Ben Mahamoud O, Takrouni ML, Zouba A, Khoualdia O, Bové JM, Duran-Vila N (2007) Manganese and brittle leaf disease of date palm trees. *J Plant Pathol* 89:49–60
- Roberts IN, Murray PF, Caputo CP, Passeron S, Barneix AJ (2003) Purification and characterization of a subtilisin-like serine protease induced during the senescence of wheat leaves. *Physiol Plantarum* 118:483–490
- Saadi I, Namsi A, Ben Mahamoud O, Takrouni ML, Zouba A, Bové JM, Duran-Vila N (2006) First report of ‘maladie des feuilles cassantes’ (brittle leaf disease) of date palm in Algeria. *Plant Pathol* 55:572
- Saidi MN, Ladouce N, Hadhri R, Grima-Pettenati J, Drira N, Gargouri-Bouzd R (2010) Identification and characterization of differentially expressed ESTs in date palm leaves affected by brittle leaf disease. *Plant Sci* 179:325–332
- Saidi MN, Jbir R, Ghorbel I, Namsi A, Drira N, Gargouri-Bouzd R (2012) Brittle leaf disease induces an oxidative stress and decreases the expression of manganese-related genes in date palm (*Phoenix dactylifera* L.). *Plant Physiol Biochem* 50:1–7
- Salvucci ME (2008) Association of Rubisco activase with chaperonin-60b: a possible mechanism for protecting photosynthesis during heat stress. *J Exp Bot* 59:1923–1933
- Schevchenko A, Wilm M, Vorm O, Mann M (1996) Mass spectrometric sequencing of proteins silver-stained polyacrylamide gels. *Anal Chem* 68:850–858
- Seidler A (1996) The extrinsic polypeptides of photosystem II. *Biochim Biophys Acta* 1277:35–60
- Sghaier-Hammami B, Valledor L, Noureddine D, Jorrín Novo JV (2009a) Proteomic analysis of the development and germination of date palm (*Phoenix dactylifera* L.) zygotic embryos. *Proteomics* 9:2543–2554
- Sghaier-Hammami B, Drira N, Jorrín Novo JV (2009b) Comparative 2-DE proteomic analysis of date palm (*Phoenix dactylifera* L.) somatic and zygotic embryos. *J Proteomics* 73:161–177
- Sghaier-Hammami B, Jorrín-Novo JV, Gargouri-Bouzd R, Drira N (2010) Abscisic acid and sucrose increase the protein content in date palm somatic embryos, causing changes in 2-DE profile. *Phytochemistry* 71:1223–1236
- Sghaier-Hammami B, Redondo-López I, Maldonado-Alconada AM, Echevarría-Zomeño S, Jorrín-Novo JV (2012) A proteomic approach analysing the *Arabidopsis thaliana* response to virulent and avirulent *Pseudomonas syringae* strains. *Acta Physiol Plant* 34:905–922
- Sharov AA, Dudekula DB, Ko MS (2005) A web-based tool for PC and significance analysis of microarray data. *Bioinformatics* 21:2548–2549
- Sturn A, Quackenbush J, Trajanoski Z (2002) Genesis: cluster analysis of microarray data. *Bioinformatics* 18:207–208
- Triki MA, Zouba A, Khoualdia O, Ben Mahamoud O, Takrouni ML, Garnier M, Bové JM, Montarone M, Poupet A, Flores R, Daròs JA, Fadda ZGN, Moreno P, Duran-Vila N (2003) ‘Maladie des feuilles cassantes’ or brittle leaf disease of date palms in Tunisia: biotic or abiotic disease? *J Plant Pathol* 85:71–79
- Valledor L, Jorrín JV (2011) Back to the basics: maximizing the information obtained by quantitative two dimensional gel electrophoresis analyses by an appropriate experimental design and statistical analyses. *J Proteomics* 74:1–18
- Wang W, Vignani R, Scali M, Cresti M (2006) A universal and rapid protocol for protein extraction from recalcitrant plant tissues for proteomic analysis. *Electrophoresis* 27:2782–2786
- Zhang YM, Zhao J, Xiang Y, Bian X, Zuo Q, Shen Q, Gai J, Xing H (2011) Proteomics study of changes in soybean lines resistant and sensitive to *Phytophthora sojae*. *Proteome Sci* 9:52